small NANO MICRO

Nanotubes

Salt Rejection and Water Transport Through Boron Nitride Nanotubes

Tamsyn A. Hilder, Daniel Gordon, and Shin-Ho Chung*

***N**anotube-based water-purification devices have the potential to transform the field of desalination and demineralization through their ability to remove salts and heavy metals without significantly affecting the fast flow of water molecules. Boron nitride nanotubes have shown superior water flow properties compared to carbon nanotubes, and are thus expected to provide a more efficient water purification device. Using molecular dynamics simulations it is shown that a (5, 5) boron nitride nanotube embedded in a silicon nitride membrane can, in principle, obtain 100% salt rejection at concentrations as high as 1 M owing to a high energy barrier while still allowing water molecules to flow at a rate as high as 10.7 water molecules per nanosecond (or 0.9268 L m^{-2} h^{-1}). Furthermore, ions continue to be rejected under the influence of high hydrostatic pressures up to 612 MPa. When the nanotube radius is increased to 4.14 Å the tube becomes cation-selective, and at 5.52 Å the tube becomes anion-selective.*

Keywords:
- desalination
- filters
- membranes
- molecular dynamics
- nanotubes

1. Introduction

Currently, approximately 25% of the world's population is affected by water shortages.[1] With population growth and climate change limiting the world's fresh water stores, desalination (removing salts) and demineralization (removing heavy metals) from seawater is fast becoming a possible solution. Unfortunately, current desalination methods are expensive and inefficient as they require energies of ≈3.4 kWh m^{-3}, approximately four times the thermodynamic minimum energy required to achieve reverse osmosis or separate salt from seawater (0.8 kWh m^{-3}).[2] There is a genuine and urgent need to make the process of desalination more effective and less costly than the currently available method. Nanotube-based water purification devices have the potential to transform the field of desalination and demineralization.

Kalra et al.[3] showed that a hexagonally packed array of (6, 6) carbon nanotubes obtained flow rates of 5.8 water molecules per ns using molecular dynamics (MD) and osmotically driven transport. While carbon nanotubes have been shown to reject salt ions, Fornasiero et al.[4] show that this rejection breaks down when the ion concentration increases above 1 mM. Beyond 10 mM no ions are rejected. Contrary to Fornasiero et al.,[4] the (5, 5) and (6, 6) hexagonally packed carbon nanotubes studied by Corry[5] using MD exhibited 100% salt rejection for a concentration of 250 mM and a pressure of 208 MPa with flow rates of approximately 10.4 and 23.3 water molecules per ns, respectively.

The presence of partial charges on the carbon nanotube has a significant effect on conduction and acceptance of charged molecules.[6,7] Majumder et al.[6] place negatively charged functional groups at the carbon-nanotube tips and find that this significantly increases the flux of positive ions, although this effect is reduced at higher ionic concentration.[6] Similarly, Joseph et al.[7] show that placing partial charges on the rim atoms of a carbon nanotube significantly increases ion occupancy.

Single-walled nanotubes may be manufactured from a range of materials other than carbon, for example, boron nitride and silicon.[8] In comparison to carbon nanotubes, boron nitride nanotubes exhibit improved electronic properties, high chemical stability, improved biocompatibility, and high resistance to oxidation at high temperatures.[9] Furthermore, boron nitride nanotubes have shown superior water permeation properties compared to carbon nanotubes of similar diameter and length.[10–12] Water molecules inside a (5, 5)

[*] Dr. T. A. Hilder, Dr. D. Gordon, Prof. S.-H. Chung
Computational Biophysics Group, Research School of Biology
Australian National University, ACT 0200 (Australia)
E-mail: tamsyn.hilder@anu.edu.au

Supporting Information is available on the WWW under http://www.small-journal.com or from the author.

DOI: 10.1002/smll.200900349

boron nitride nanotube form a single-file chain and the nanotube conducts at a rate of 5.1 molecules per ns.[10] In contrast, the (5,5) carbon nanotube barely fills with water. Each boron and nitrogen atom forming the boron nitride nanotube acquires a partial charge, and these atoms become further polarized in the presence of water. Won and Aluru[11] use density functional theory to determine these partial charges and find that although the partial charges improve the wetting behavior, there is a slight decrease in the diffusion coefficient due to the formation of hydrogen bonds between the water and nitrogen atoms.

As yet, no studies exist that investigate the conduction and rejection of ions in boron nitride nanotubes. Here we show that a (5, 5) boron nitride nanotube embedded in a silicon nitride membrane[13] can, in principle, obtain 100% salt rejection at concentrations as high as 1 M and that water molecules continue to traverse the tube at a rate as high as 10 water molecules per ns. These theoretical predictions illustrate that a single boron nitride nanotube embedded in silicon nitride is capable of mimicking the biological water channel aquaporin-1, which obtains flow rates of approximately 3 water molecules per ns. It is hoped that such results may facilitate future development in the potential use of nanotubes for desalination and that as the technology improves these nanotubes may become more viable as a solution to desalination.

2. Results and Discussion

2.1. Salt Rejection and Water Structure

We perform MD simulations on open-ended, finite-length boron nitride nanotubes of various radii embedded in a silicon nitride matrix, as illustrated in Figure 1. Silicon nitride membranes 2–3-μm thick with carbon nanotube pores 13 to 20 Å in diameter have been successfully manufactured[13,14] with a pore density of 2.5×10^{11} cm^{-2}. The authors[14] note that there is a large uncertainty in the determination of this pore density. The value quoted above was derived from the plan-view of transmission electron microscopy images of 0.2 μm by 0.2 μm. Therefore, we assume that it is possible to manufacture silicon nitride membranes with boron nitride nanotube pores. In contrast to polymer membranes, silicon nitride membranes exhibit negligible molecular permeability,[13] making them a suitable membrane material.

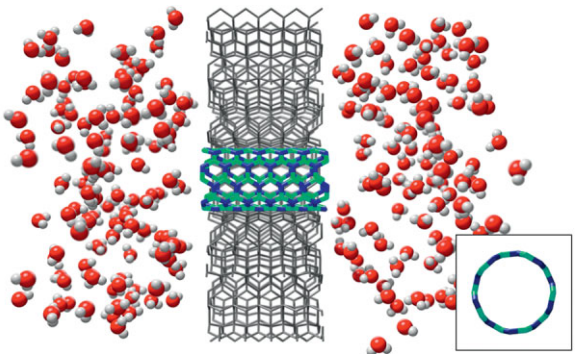

Figure 1. Visualization of a boron nitride nanotube-embedded silicon nitride membrane. The boron nitride nanotube is shown inside a silicon nitride matrix between two water reservoirs. Note that for clarity not all water molecules are shown. The inset illustrates the boron nitride nanotube pore.

We consider open-ended (5,5), (6,6), (7,7), and (8,8) boron nitride nanotubes with a length of approximately 14 Å and radii of 3.45, 4.14, 4.83, and 5.52 Å, respectively. Here we study only armchair-type nanotubes (n, n) to minimize computational time. Similarly sized zigzag nanotubes (n, 0) are likely to display similar energy profiles and selectivity. For example, we investigated the (9, 0) boron nitride nanotube, which has a radius close to that of the (5, 5) nanotube (3.59 Å), and found a similar free-energy profile for sodium ions. The boron nitride nanotubes are constructed from a hexagonal array[15] of alternating boron and nitrogen atoms rolled up to form a tubular structure[16] (see Experimental Section). In reality, the nitrogen atoms shift outwards[17] due to the electronic structure by approximately 0.061 Å. We find the effect of shifting the nitrogen atoms to be negligible, and thus did not include this adjustment for the remainder of the simulations.

It is uncertain which values for the partial charges on boron and nitrogen atoms are the most suitable to properly represent the electrostatics of the boron nitride nanotube. In a previous study Won and Aluru[11] use density functional theory and determine partial charges on the boron and nitrogen atoms as $\pm 0.4\,e$ without water, and ±1.05 e in water for the (5, 5) boron nitride nanotube. Similarly, for the (6, 6) boron nitride nanotube they determine a partial charge of $\pm 0.39\,e$ without water and $\pm 0.76\,e$ in water. They do not investigate the (7, 7) and (8, 8) boron nitride nanotubes. We confirm their results for the (5, 5) boron nitride nanotube without water using Gaussian03[18] and CPMD[19] (unpublished). In reality, the charges on both the water molecules and the boron nitride nanotube will be modified through their electrostatic interaction. The basis set used by Won and Aluru[11] to determine the partial charges exaggerates the dipole moment by 10%–20% and thus incorporates the amount of polarization that would be expected in aqueous solutions.[20] MD does not adjust the charges of water and thus by using the value of the partial charge in water for the boron nitride nanotube there may be some double counting of electrostatic interactions. Therefore, we investigate the sensitivity of our results to changes in partial charge by assigning both the charge without water and with water.[11]

The effect of water structure in aiding or hindering conduction is investigated. All four tubes studied accept water molecules into their interior. As the nanotube radius increases, the water structure formed within the tube changes from a single-file chain to an ordered water tube. Moreover, as the tube radius increases, the water structure within the tube begins to influence salt rejection.

The (5, 5) and (6, 6) boron nitride nanotubes both exhibit a single-file chain of water molecules as illustrated in Figure 2 where the x-axis is the radial distance from the nanotube center. When a sodium ion is placed inside the nanotube the water structure surrounding the ion is different within each tube. For the (5, 5) tube the sodium ion is solvated by two water molecules, one on either side of the ion, whereas for the (6, 6) tube there is sufficient space for the sodium ion to shift off center

NANO MICRO small

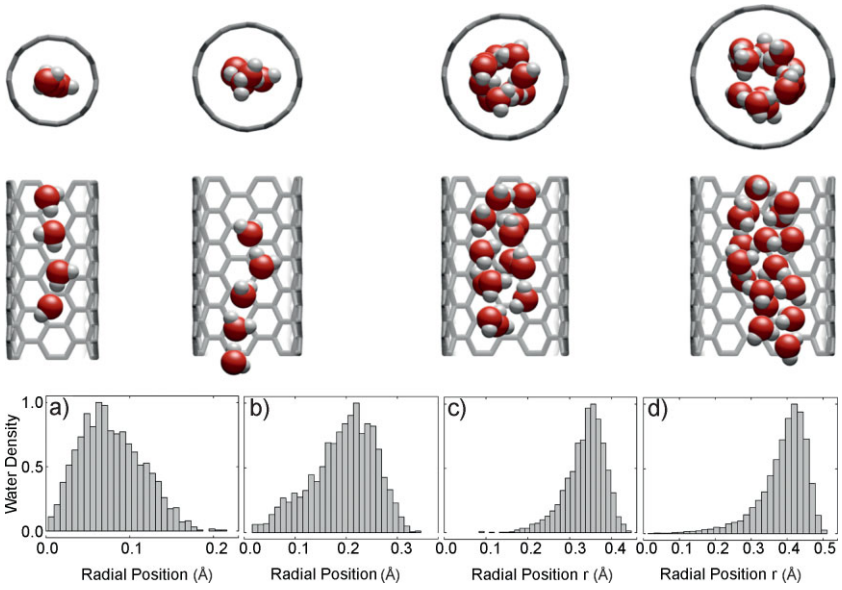

Figure 2. Water molecules inside boron nitride nanotubes. Bottom: The radial water density distribution of water molecules, where the *x*-axis represents the radial position from the center of the nanotube. Top: The average position of water from MD simulations for a) (5, 5), b) (6, 6), c) (7, 7), and d) (8, 8) tubes.

and thus be solvated by three water molecules, as illustrated in Figure 3b and c, respectively. The sodium ion is rejected from the (5, 5) tube due to the cost of dehydration. In bulk water ions are usually bound by between four and six water molecules, and these ions are called solvated or hydrated ions. The cost of dehydration is the amount of energy required to remove water molecules from this tightly bound hydration shell.[21] As shown in Figure 3a, the potential mean force (PMF), or free energy, of a sodium ion for the (5, 5) boron nitride nanotube has a large energy barrier regardless of partial charge used, whereas the (6, 6) boron nitride nanotube has a small energy well. Although there are only three waters solvating the sodium ion inside the (6, 6) nanotube there is no energy barrier for the sodium ion to overcome. We speculate that this surprising result is due to the water structure within the nanotube and the unique electrostatics of the boron nitride nanotube.

On examination of the PMF for all four tubes studied, the (5, 5) boron nitride nanotube is found to be the only tube that rejects both sodium and chloride ions, whereas all other tubes investigated accept either sodium or chloride. A similar observation is made for the (5, 5) and (6, 6) carbon nanotube.[3,5] The (5, 5) boron nitride nanotube rejects chloride ions primarily due to a sieving affect since the tube diameter is too small to accept the ion into its interior. There is also a high energy barrier for entry of a chloride ion into the (6, 6) tube due to the cost of dehydration. Thus, the (6, 6) tube has the potential to be used as a cation-selective nanodevice, mimicking the function of the gramicidin channel.[22]

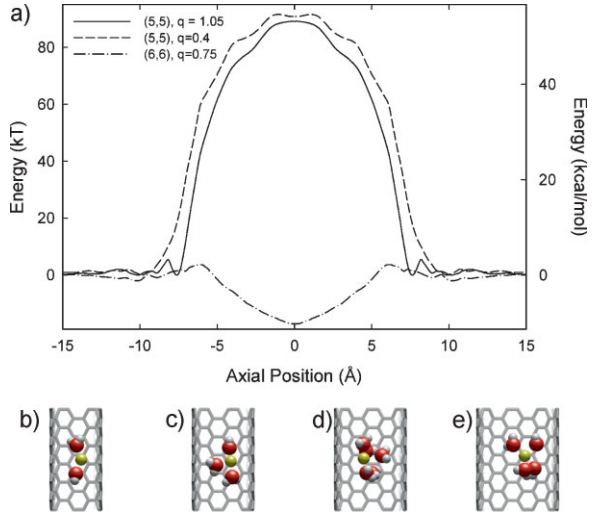

Figure 3. Sodium ion inside a boron nitride nanotube. a) The free energy for Na^+ inside a boron nitride nanotube of type (5, 5) with a partial charge $\pm 1.05\,e$ (—), (5, 5) with a partial charge of $\pm 0.4\,e$ (- -), and (6, 6) with a partial charge of $\pm 0.76\,e$ (- · -). The structure of water surrounding a sodium ion in a b) (5, 5), c) (6, 6), d) (7, 7), and e) (8, 8) boron nitride nanotube.

As the tube is increased to the (7, 7) nanotube, the water structure appears to spiral through the nanotube, with each water molecule having approximately three other water molecules in the first solvation shell. To form this spiral structure the water molecules shift away from the center of the tube. As the tube radius increases the water molecules shift away from the center of the nanotube. In other words, as the radius of the nanotube increases the degree of radial freedom increases (as illustrated in Figure 2). A similar observation is made for carbon nanotubes.[5] The (7, 7) nanotube is shown to accept sodium ions but reject chloride ions due to a large energy barrier.

The water structure within the (8, 8) nanotube resembles a tube with four sides forming square rings with four O–H bonds. Highly ordered structures of water have been observed within carbon nanotubes, and it has been suggested that these structures are n-gonal rings forming ice nanotubes.[23,24] This water structure is found to affect the acceptance or rejection of ions in various cases. The (8, 8) boron nitride nanotube has a large enough radius to accept both sodium and chloride ions, but it is shown to reject sodium ions due to a large energy barrier and accept chloride ions. This can be explained by the observation that the sodium ion disrupts the water structure in such a way that it is not favorable for the ion to enter. However, the chloride ion is accepted since it does not significantly disrupt this structure. More specifically, the chloride ion almost replaces a water molecule that participates in a 4-gonal water ring within the (8, 8) nanotube whereas the water molecules must reorganize to allow for the sodium ion, thus disrupting the unique 4-gonal ring.

2.2. Water Conduction

The ability of the (5,5) boron nitride nanotube to reject both anions and cations makes it a possible candidate as a desalination device. Thus, the (5, 5) boron nitride nanotube membrane was investigated further to determine its effectiveness. To start, the entire system was equilibrated without water in the channel. The first water molecule entered the channel after only 1 ps, and the channel completely filled at 17 ps. The model was then run for 7 ns to determine the water density characteristics within the tube. Figure 4a illustrates the density of water along the axial direction within the nanotube over the 7 ns. The water molecules tend to preferentially dwell on four positions along the tube. During the 7 ns equilibration, there tend to be on average between three and four water molecules occupying the tube, as illustrated in Figure 4b. The average openness, $\langle\omega\rangle$, of the boron nitride nanotube to water conduction[25] is shown to be 0.9971, which compares well to the results of Won and Aluru.[10,11] In comparison, water chains in the (5, 5) carbon nanotube only form half the time,[5] with an average openness of 0.058.[10]

The (5, 5) boron nitride nanotube system was then run with an applied pressure ranging from 60 to 612 MPa. Beyond 612 MPa the water structure begins to break down, therefore pressures were kept below 612 MPa. Most reverse osmosis membranes currently operate at pressures under 10 MPa, and the standard operating pressure for seawater reverse osmosis membranes is 5.5 MPa (a lower pressure is needed for brackish water). We performed simulations at higher pressures to allow more conduction events to occur in a shorter simulation time, the results of which may be extrapolated to smaller pressures.[5]

Water molecules are shown to move through the boron nitride nanotube in single-file and in a concerted motion, as illustrated in Figure 5 for a pressure difference of 305.8 MPa. The best measure of efficiency for a desalination device is a measure of the ion and water conduction.[5] We define a conduction event as the average number of crossing events for the two nanotube ends (see Experimental Section). Figure 6 illustrates the conduction of water molecules against the applied pressure. The slopes of the best fit curves can be used to determine the osmotic permeability and subsequently the hopping rate. The hopping rate, obtained from the conduction versus pressure curve (see Experimental Section), was found to be 10.74 and 10.45 water molecules per ns for a partial charge $q = \pm 0.4\,e$ with ions (concentration, $c = 0.5$ M) and without ions, respectively, and 1.57 and 1.57 water molecules per ns for $q = \pm 1.05\,e$ with ions ($c = 0.5$ M) and without ions, respectively (see Supporting Information, Table S1). Assuming an effective pore radius through the (5, 5) boron nitride nanotube and utilizing the average volume of a single water molecule (see Experimental Section) a flow rate of 10.74 water molecules per ns is equivalent to a membrane flux of 0.9268 L m^{-2} h^{-1}. We also determined the conduction against pressure curve for $q = \pm 1.05\,e$ and an ion concentration of 1 M. The conduction profile did not differ significantly from that of the 0 and 0.5 M cases (see Supporting Information, Figure S1). These compare well to the biological water channel, aquaporin-1, which has a flow rate of 3 water molecules per ns[26] and to conduction rates obtained in previous studies.[10–12] Furthermore, the permeability for the (5, 5) boron nitride nanotube compares well to that obtained by Corry[5] for the (6, 6) carbon nanotube.

Similar to Majumder et al.[6] and Joseph et al.,[7] we find that partial charge has a significant effect on the conduction of both ions and water molecules (Figure 6). As with Won and Aluru,[11] we deduce that an increase in partial charge results in

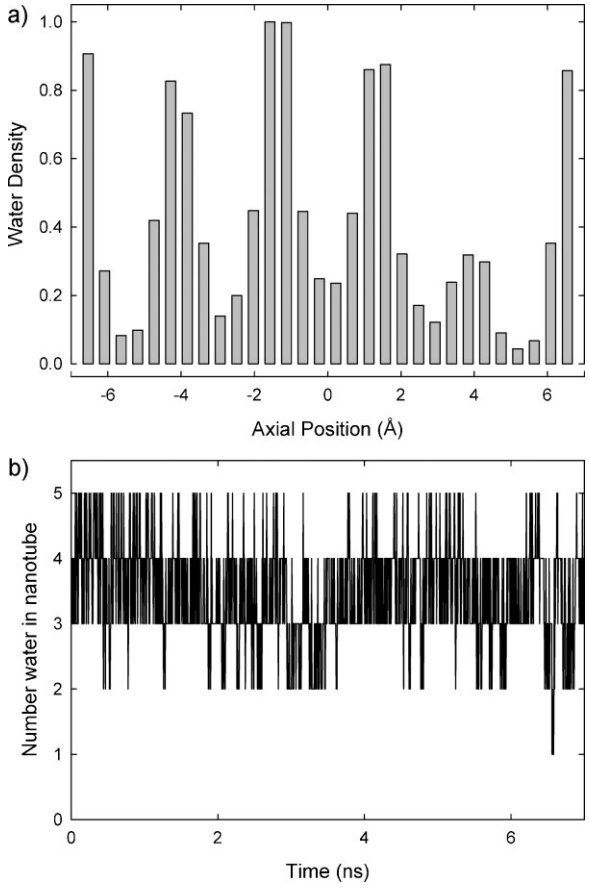

Figure 4. Water occupancy in the (5, 5) boron nitride nanotube. a) The water density along the nanotube axis. b) The number of water molecules inside the nanotube over the 7 ns simulation time.

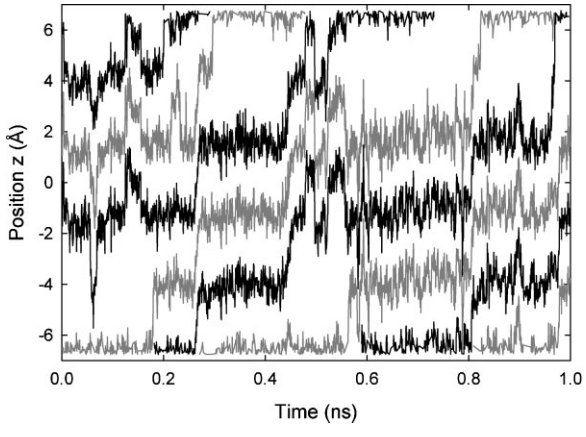

Figure 5. Positions of water during simulation. Motions of individual water molecules plotted against simulation time for a hydrostatic pressure of 305.8 MPa.

NANO MICRO small

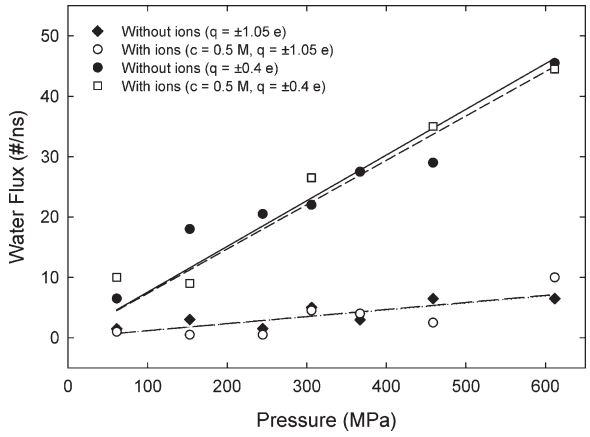

Figure 6. Conduction of water molecules through the boron nitride nanotube. Data points are direct from MD simulations and curves represent the lines of best fit, where *c* represents the ion concentration and *q* represents the partial charge on the boron and nitrogen atoms.

an increased interaction between the water molecules and the tube wall. In other words, as the charge decreases, the interaction decreases and therefore the conduction increases (Figure 6). The interaction results in the water molecules navigating to discrete positions along the tube length. As the charge is decreased we note that these discrete positions become less significant, which in turn enables a faster flow of water through the nanotube. Won and Aluru[11] suggest that this is due to a decrease in the number of hydrogen bonds formed between the water and nitrogen atoms. Thus, the conduction rates for $q = \pm 0.4$ e and $q = \pm 1.05$ e represent best and worst case scenarios, respectively. For example, the electrostatic interaction may be overestimated in the latter case and thus the obtained conduction curve represents the worst case.

With ions present in the water reservoirs at a concentration of both 0.5 and 1 M the applied pressure does not cause ions to enter or traverse the tube. This is in contrast to the investigation by Fornasiero et al.[4] on carbon nanotubes that found that the rejection of ions was concentration-dependent so that at concentrations higher than 10 mM all ions entered the nanotube. Fornasiero et al.[4] examine tubes that are 5–10 Å in radius and are thus larger than those tubes studied here. It is possible that they are observing ion chaperoning, whereby rejection is a balance between opposite electrostatic forces such that one ion chaperones the other ion through the tube. In this paper, the tube radius is such that it is too narrow for the chloride ion to enter, and thus ion chaperoning cannot occur. The presence of ions does not significantly affect the flow of water molecules, as illustrated in Figure 6. Moreover, the presence of an 80 kT energy barrier (Figure 3a) suggests 100% ion rejection is likely. Assuming 0% rejection of ions, we would expect one ion to traverse the tube every 13.9 ns (for 458.7 MPa, 1 M concentration and $\pm 1.05\,e$). Consequently, upon extending the run time to 14.5 ns, we continue to observe no ions traversing the tube. Moreover, in the 14.5 ns simulation ions reach the mouth of the tube but none enter the tube or affect water conduction.

It is possible to use the conduction curve generated from these simulations to extrapolate to smaller pressures. In doing so we can predict the flow rate at standard operating pressures (5.5 MPa for seawater) and make a comparison to products currently on the market. For example, using the same surface area we obtain a water flow rate approximately 4.2 times that of the FILMTEC SW30HR-380 premium grade seawater reverse osmosis element produced by Dow water solutions.[27] This figure is based on a pore density of 2.5×10^{11} cm^{-2}, and thus a higher pore density may further improve the efficiency. For example, increasing the pore density by 25% generates flow rates 5.2 times that of the FILMTEC SW30HR-380. In comparison, the (5, 5) carbon nanotube membrane obtains a flow rate approximately 2.42 times that of the FILMTEC SW30HR-380 element.[5] Other work has reported water flow rates orders of magnitude larger than theoretical predictions.[14] However, this work investigates the flow of water through much larger nanotubes than those presented here (radii of approximately 8 Å compared to less than 5.52 Å). As a result these larger nanotubes will allow larger water flow rates. In addition, previous theoretical studies[3–5] often investigate the nanotubes in a hexagonally packed array, which will also increase the amount of water that can flow across the membrane.

The mechanical integrity of the membrane is critical for their subsequent use as desalination devices. A limitation of the current membrane is that operating pressures are limited since silicon nitride is a ceramic material, and is therefore brittle in nature.[13] Holt et al.[14] propose a method to fabricate crack-free membranes with carbon nanotube pores, thus reducing the risk of failure. Furthermore, boron nitride nanotubes may provide reinforcement to the silicon nitride matrix[13,28] similar to their use in glass composites where they exhibit 90% strength improvement.[29] To withstand a standard operating pressure of 5.5 MPa, a boron nitride nanotube-embedded silicon nitride membrane 1.4-nm-thick must have an area less than 2.64×10^{-3} μm^2 (see Experimental Section). Using a membrane area of 35 m^2 (that of FILMTEC SW30HR-380[27]) we obtain a maximum operating pressure ΔP_{max} of 0.05 Pa. Thus, to improve mechanical strength it may be necessary to either increase the membrane thickness, use an alternate embedding material such as polycarbonate,[14,30] or apply a thin coating to the membrane such as porous silicon.[31] We note that increasing the membrane thickness, or tube length, from 14 to 21 Å has no significant effect on the conduction of water (see Supporting Information, Figure S1). Thus, casting the proposed membrane on a porous silicon support[31] could improve the membrane strength at no significant cost to water conduction provided that the minimum pore size of the porous support is larger than the critical pore size for conduction of water molecules (≈7 Å).[5,32]

3. Conclusions

We show that, in principle, a boron nitride nanotube-embedded silicon nitride membrane can conduct water molecules while rejecting ions, thus producing an efficient desalinator. The (5, 5) boron nitride nanotube membrane is

shown to reject both anions and cations while conducting water at a rate of 1.6–10.7 water molecules per ns. Salt rejection is shown to be a result of both nanotube radius and the water structure within the nanotube. When the nanotube radius is increased to 4.14 Å (a (6, 6) boron nitride nanotube) the tube becomes cation-selective, and at 5.52 Å (an (8, 8) tube) the tube becomes anion-selective. The water structure forms a single-file chain in the (5,5) and (6,6) tubes and develops into an ordered spiral and a 4-gonal tube for the (7, 7) and (8, 8) tubes, respectively. To obtain water that is fit for human consumption from seawater there must be >95% salt rejection.[5] We show that the (5, 5) boron nitride nanotube-embedded silicon nitride membrane can, in principle, achieve 100% salt rejection at concentrations as high as 1 M.

4. Experimental Section

Boron nitride nanotube construction: Boron nitride nanotubes were constructed from a hexagonal array[15] of alternating B and N atoms rolled up to form a tubular structure[16] similar to the carbon nanotube. We used a B–N bond distance of 1.446 Å.[11] Similar to carbon nanotubes, the boron nitride nanotube is defined by its chiral vector, $\boldsymbol{C} = (n, m)$. We consider only armchair tubes that are defined by $\boldsymbol{C} = (n, n)$. The boron nitride nanotubes were constructed using the physical parameters of a carbon nanotube[33] and unit cell parameters for the boron nitride nanotube. To generate the boron nitride nanotube a simple atom substitution of carbon atoms to boron or nitrogen atoms was then performed and new pdb and psf files were generated. The Lennard–Jones constants for boron and nitrogen atoms were obtained from Won and Aluru.[10]

MD simulations: MD simulations were performed using NAMD[34] and visualized using VMD.[35] The MD domain consisted of a boron nitride nanotube, a silicon nitride matrix, water, and sodium and chloride ions. The nanotube is fixed in the silicon nitride membrane and separates two reservoirs containing water and ions (Figure 1). The silicon nitride matrix was constructed using the methodology outlined in the bionanotechnology VMD and NAMD online tutorial.[36] The simulation box for all runs was approximately $4.5 \times 4 \times 6.4\ \mathrm{nm}^3$. The system was replicated periodically in all three dimensions. The simulation box contained approximately 1 200 water molecules and 6–7 sodium and chloride ion pairs for an ion concentration of 0.5 M. In addition, the effect of concentration was examined by increasing the concentration to 1 M, or 11 sodium and chloride ion pairs. CHARMM27[37] force field parameters and the TIP3 water model was used for all simulations.

The four nanotubes were also run in isolation to examine the importance of water structure under a constant temperature for 76 ps in order to let the water molecules enter the tube. During this time the water molecules enter the nanotube from the outside reservoirs and reach equilibrium. The reservoirs were then removed and the remaining water molecules were constrained within the nanotubes and a subsequent equilibration was run for 200 ps to establish the water structure within the tubes.

Free-energy calculations: The simulation was performed at a constant temperature of 310 K. Initially the system was equilibrated for 51 ps to a constant temperature of 310 K and constant pressure of 1 bar. The PMF of both a sodium and chloride ion moving through each of the four nanotubes was calculated using umbrella sampling. For all runs the silicon nitride matrix and the boron nitride nanotube were restrained with a harmonic constraint of 1.0 and 0.5 kcal mol^{-1} Å^{-1}, respectively. The ion was moved through positions, z_0 from −15 to 0 in 0.5 Å increments and held in position using a harmonic constraint of 0.5 kcal mol^{-1} Å^{-1}. Each window was run for a total of 0.5 ns. Runs were then analyzed using the weighted-histogram-analysis method[38] using the implementation by Grossfield.[39]

Hydrostatic pressure: A pressure was applied both with and without ions to the (5, 5) boron nitride nanotube system. This pressure was created by applying a constant force f in the positive z direction to all water molecules in the region with an absolute z-coordinate greater than 16 Å to create a pressure difference across the membrane. The pressure difference, ΔP, is given by $\Delta P = nf/A$, where n is the number of water molecules with an applied force and A is the cross-sectional area of the membrane.[5,40,41] The pressure difference was varied from 60 to 612 MPa and was applied to 433 and 439 water molecules for the case where ions were included and excluded. The system was then run for 1 ns at a constant temperature of 310 K with harmonic constraints of 1.0 and 0.5 kcal mol^{-1} Å^{-1} applied to the silicon nitride membrane and boron nitride nanotube, respectively. Unlike in desalination, the ions were present in the water reservoirs on either side of the membrane and the rejection of ions was investigated under an applied pressure. This is a more simple method for simulating the conditions an ion will experience under osmotic pressure and has been used previously.[5]

Silicon nitride is a ceramic material, and therefore there is a limit to the amount of pressure a silicon nitride membrane can withstand. The theoretical maximum pressure difference, $\Delta P_{\max}$ that a solid silicon nitride membrane can withstand prior to rupture[42] is given by

$$\Delta P = 0.29K\left(\frac{t_m}{r_m}\right)\sigma_{yield}\sqrt{\frac{\sigma_{yield}}{E}} \quad (1)$$

where K is the non-perforated fraction of the membrane, t_m is the membrane thickness, r_m is the membrane radius, σ_{yield} is the yield stress of the material, and E is the Young's modulus. For bulk silicon nitride we have $\sigma_{yield} = 4$ GPa and $E = 385$ GPa.[13,42] The osmotic permeability p_f was determined by[41]

$$\frac{j_n}{\Delta P} = \frac{p_f}{k_B T} \quad (2)$$

where j_n is the number of water molecules per second that flow through the nanotube, k_B is Boltzmann's constant, and T is the absolute temperature. The value of $j_n/\Delta P$ is equivalent to the best fit slope of the conduction versus pressure curve. The conduction, j_n was measured as the average number of crossing events for the two nanotube ends. In other words, a molecule moving from outside to inside the nanotube in a positive or negative direction increases the total number of crossing events by +1 or −1, respectively. Similarly, moving from inside to outside the nanotube in a positive or negative direction increases the total number of crossing events by +1 or −1, respectively. The resulting conduction

NANO MICRO small

is then one half of the total number of crossing events, or the average number of crossing events.

Once the osmotic permeability is known, the number of hops per second, D_n, can be determined by $p_f = \upsilon_w D_n$,[40] where υ_w is the average volume of a single water molecule and is given by V_W/N_A and V_W is $18\,cm^3\,mol^{-1}$ and N_A is Avogadro's number (6.023×10^{23}). It is important to note that D_n is also known as the hopping rate or the diffusion coefficient of n, where n is the net amount of water permeation.[40] The number of hops is equivalent to the number of water molecules when the flow through the tube is single-file, since one hop results in one water molecule exiting the tube.

Acknowledgements

We gratefully acknowledge the support from the National Health and Medical Research Council. The authors wish to acknowledge helpful comments, discussion, and assistance from Ganesh Venkateshwara, Rui Yang, Alistair Rendell, Andrey Bliznyuk, and Silvie Ngo. We acknowledge the use of the Australian National University Supercomputer Facility and Rhys Hawkins from the Visualization Lab at the Australian National University.

[1] J. Mullins, "Cheap Desalination," http://www.newscientist.com/blog/invention/2008/01/cheap-desalination.html (accessed January 2008).
[2] R. Semiat, *Environ. Sci. Technol.* **2008**, *42*, 8193–8201.
[3] A. Kalra, S. Garde, G. Hummer, *Proc. Natl. Acad. Sci. USA* **2003**, *100*, 10175–10180.
[4] F. Fornasiero, H. G. Park, J. K. Holt, M. Stadermann, C. P. Grigoropoulos, A. Noy, O. Bakajin, *Proc. Natl. Acad. Sci. USA* **2008**, *105*, 17250–17255.
[5] B. Corry, *J. Phys. Chem. B* **2008**, *112*, 1427–1434.
[6] M. Majumder, N. Chopra, B. J. Hinds, *J. Am. Chem. Soc.* **2005**, *127*, 9062–9070.
[7] S. Joseph, R. J. Mashi, E. Jakobsson, N. R. Aluru, *Nano Lett.* **2003**, *3*, 1399–1403.
[8] P. Fortina, L. J. Kricka, S. Surrey, P. Grodzinski, *Trends Biotechnol.* **2005**, *23*, 168–173.
[9] V. L. Solozhenko, A. G. Lazarenko, J.-P. Petitet, A. V. Kanaev, *J. Phys. Chem. Solids* **2001**, *62*, 1331–1334.
[10] C. Y. Won, N. R. Aluru, *J. Am. Chem. Soc.* **2007**, *129*, 2748–2749.
[11] C. Y. Won, N. R. Aluru, *J. Phys. Chem. C* **2008**, *112*, 1812–1818.
[12] M. E. Suk, A. V. Raghunathan, N. R. Aluru, *Appl. Phys. Lett.* **2008**, *92*, 133120.
[13] J. K. Holt, A. Noy, T. Huser, D. Eaglesham, O. Bakajin, *Nano Lett.* **2004**, *4*, 2245–2250.
[14] J. K. Holt, H. G. Park, Y. Wang, M. Stadermann, A. B. Artyukhin, C. P. Grigoropoulos, A. Noy, O. Bakajin, *Science* **2006**, *312*, 1034–1037.
[15] P. Widmayer, H.-G. Boyen, P. Ziemann, P. Reinke, P. Oelhafen, *Phys. Rev. B: Condens. Matter Mater. Phys.* **1999**, *59*, 5233–5241.
[16] M. Ishigami, S. Aloni, A. Zettl, *AIP Conference Proceedings for 12th International Conference STM'03* **2003**, *696*, 94–99.
[17] N. Park, J. Cho, H. Nakamura, *J. Phys. Soc. Jpn.* **2004**, *73*, 2469–2472.
[18] Gaussian 03, Revision C.02, M. J. Frisch, G. W. Trucks, H. B. Schlegel, G. E. Scuseria, M. A. Robb, J. R. Cheeseman, J. A. Montgomery, Jr, T. Vreven, K. N. Kudin, J. C. Burant, J. M. Millam, S. S. Iyengar, J. Tomasi, V. Barone, B. Mennucci, M. Cossi, G. Scalmani, N. Rega, G. A. Petersson, H. Nakatsuji, M. Hada, M. Ehara, K. Toyota, R. Fukuda, J. Hasegawa, M. Ishida, T. Nakajima, Y. Honda, O. Kitao, H. Nakai, M. Klene, X. Li, J. E. Knox, H. P. Hratchian, J. B. Cross, V. Bakken, C. Adamo, J. Jaramillo, R. Gomperts, R. E. Stratmann, O. Yazyev, A. J. Austin, R. Cammi, C. Pomelli, J. W. Ochterski, P. Y. Ayala, K. Morokuma, G. A. Voth, P. Salvador, J. J. Dannenberg, V. G. Zakrzewski, S. Dapprich, A. D. Daniels, M. C. Strain, O. Farkas, D. K. Malick, A. D. Rabuck, K. Raghavachari, J. B. Foresman, J. V. Ortiz, Q. Cui, A. G. Baboul, S. Clifford, J. Cioslowski, B. B. Stefanov, G. Liu, A. Liashenko, P. Piskorz, I. Komaromi, R. L. Martin, D. J. Fox, T. Keith, M. A. Al-Laham, C. Y. Peng, A. Nanayakkara, M. Challacombe, P. M. W. Gill, B. Johnson, W. Chen, M. W. Wong, C. Gonzalez, J. A. Pople, Gaussian, Inc, Wallingford CT, 2004.
[19] CPMD V3.13, IBM Corp **1990–2008**, MPI für Festkörperforschung Stuttgart **1997–2001**.
[20] W. Cornell, "Charge Fitting Philosophy," in: *AMBER User Manual*, Carleton University, http://cns0.carleton.ca/amber/AMBER-sh-19.03.html (accessed February 2008).
[21] J. N. Israelachvili, *Intermolecular and Surface Forces*, Academic Press, London **1985**.
[22] O. S. Andersen, R. E. Koeppe, II, B. Roux, in *Biological Membrane Ion Channels: Dynamics, Structure, and Applications* (Eds: S.-H. Chung, O. S. Andersen, V. Krishnamurthy), Springer, New York **2007**, pp. 33–80.
[23] K. Koga, R. D. Parra, H. Tanaka, X. C. Zeng, *J. Chem. Phys.* **2000**, *113*, 5037–5040.
[24] K. Koga, R. D. Parra, H. Tanaka, X. C. Zeng, *Nature* **2001**, *412*, 802–805.
[25] O. Beckstein, P. C. Biggin, M. S. P. Sansom, *J. Phys. Chem. B* **2001**, *105*, 12902–12905.
[26] P. Agre, *Angew. Chem. Int. Ed.* **2004**, *43*, 4278–4290.
[27] Dow water solutions, http://www.dow.com/liquidseps/prod/sw30hr_380.htm (accessed January 2009).
[28] Q. Huang, Y. Bando, X. Xu, T. Nishimura, C. Zhi, C. Tang, F. Xu, L. Gao, D. Golberg, *Nanotechnology* **2007**, *18*, 485706.
[29] N. P. Bansal, J. B. Hurst, S. R. Choi, *J. Am. Ceram. Soc.* **2006**, *89*, 388–390.
[30] P. Ball, *New Scientist* **2008**, *2691*, 33–35.
[31] C. J. Chearer, K. T. Constantopoulos, N. H. Voelcker, J. G. Shapter, A. V. Ellis, *Proceedings of the SPIE* **2008**, *7267*, 26701–11.
[32] T. A. Hilder, J. M. Hill, *J. Nanosci. Nanotechnol.* **2009**, *9*, 1403–1407.
[33] M. S. Dresselhaus, G. Dresselhaus, R. Saito, *Carbon* **1995**, *33*, 883–891.
[34] L. Kale, R. Skeel, M. Bhandarkar, R. Brunner, A. Gursoy, N. Krawetz, J. Phillips, A. Shinozaki, K. Varadarajan, K. Schulten, *J. Comp. Phys.* **1999**, *151*, 283–312; NAMD, http://www.ks.uiuc.edu/Research/namd/ (accessed August 2008).
[35] W. Humphrey, A. Dalke, K. Schulten, *J. Molec. Graphics* **1996**, *14*, 33–38; VMD, http://www.ks.uiuc.edu/Research/vmd/ (accessed August 2008).
[36] University of Illinois, Urbana-Champaign, Beckman Institute for Advanced Science and Technology, Theoretical and Computational Biophysics Group. "Bionanotechnology tutorial," http://www.ks.uiuc.edu/Training/Tutorials/science/bionano/bionanotutorial.pdf (accessed July 2008).
[37] a) B. R. Brooks, R. E. Bruccoleri, B. D. Olafson, D. J. States, S. Swaminathan, M. Karplus, *J. Comp. Chem.* **1983**, *4*, 187–217; b) A. D. MacKerell, Jr, B. Brooks, C. L. Brooks, III, L. Nilsson, B. Roux, Y. Won, M. Karplus, in *The Encyclopedia of Computational*

Chemistry, Vol. *1*(Eds.: P. V. R. Schleyer, P. R. Schreiner, N. L. Allinger, T. Clark, J. Gasteiger, P. Kollman, H. F. Schaefer, III, John Wiley & Sons, Chichester **1998**, pp. 271–277.
[38] Kumar, S Schaefer,, J. M. Rosenberg, D. Bouzida, R. H. Swendsen, P. A. Kollman, *J. Comp. Chem.* **1995**, *16*, 1339–1350.
[39] A. Grossfield, An implementation of WHAM: the weighted histogram analysis method, http://membrane.urmc.rochester.edu/Software/WHAM/WHAM.html (accessed August 2008).
[40] F. Zhu, E. Tajkhorshid, K. Schulten, *Phys. Rev. Lett.* **2004**, *93*, 224501.
[41] F. Zhu, E. Tajkhorshid, K. Schulten, *Biophy. J.* **2004**, *86*, 50–57.
[42] H. D. Tong, H. V. Jansen, V. J. Gadgil, C. G. Bostan, E. Berenschot, C. J. M. van Rijn, M. Elwenspoek, *Nano Lett.* **2004**, *4*, 283–287.

Received: February 27, 2009
Revised: May 15, 2009
Published online: July 6, 2009

